PERFORMANCE ASSESSMENT METRICS FOR LINE-INFRASTRUCTURE MONITORING WITH MULTI-SENSOR SAR DATA

Ling Chang[*]*, Rolf P.B.J. Dollevoet*[†] *and Ramon F. Hanssen*[†]

[*]University of Twente; [†]Delft University of Technology

ABSTRACT

Satellite radar interferometry (InSAR) has been used to monitor the structural health of line-infrastructure (e.g. railways, bridges, dams and dikes) in recent years. This enables the retrieval of millimeter-level changes in the line-infrastructure geometry on a bi-weekly basis. However, InSAR is an opportunistic method for which the location of the measurements (coherent scatterers) cannot be guaranteed, and the quality of the InSAR products vary from one case to another. Particularly, this is due to the orientation of the line-infrastructure relative to the satellite position, and its expected deformation magnitude and direction. Hence, the InSAR applicability and performance quality is not uniform. In operational situations, this tends to make asset managers skeptical about the potential of InSAR application on these assets. In this work, following [1] we develop new standard InSAR products for line-infrastructure monitoring, provide tools for predicting optimal multi-sensor SAR data combinations, and propose generic a priori performance assessment metrics for line-infrastructure. These products and metrics are tested on the Dutch railway line-infrastructure asset.

Index Terms— Line-infrastructure, multi-sensor SAR.

1. INTRODUCTION

In recent years, there has been an increasing interest in satellite-based line infrastructure deformation monitoring, e.g. [2, 3, 4]. Such satellite-based technologies, i.e. satellite radar interferometry techniques (InSAR) [5, 6], provide a less laborious, effective and economic way for continuously observing the stability and safety of line infrastructure. InSAR works in all weather and all environments, and can remotely detect sub-centimeter-scale movements, relative between two locations, over time spans of days to years, see e.g. [7] or [8]. A limiting factor for interpreting such InSAR measurements is that they are only sensitive in the satellite line-of-sight (LOS) direction. It is impossible, for a satellite with a single view geometry, to estimate the ground targets' movements in three dimensions when no additional information is available [9, 10].

[*]Contact email: ling.chang@utwente.nl

Practically, a harsh assumption that the deformation in the vertical direction is predominant can be considered, thereby the LOS deformation can be projected to the vertical direction. Although there are some classes of problems where this assumption may be fair, as the many successful InSAR applications in literature show [11, 12, 13, 14], such an assumption does not hold for all cases, see e.g. [15, 16, 17]. The problem is that in practice we don't know, and professional asset managers do

Typically, for line infrastructure, both horizontal and vertical movements occur. For instance, ground water movements, soil compaction, traffic loads and the interaction between neighboring structures contribute to the permanent settlement in the vertical direction [18], and also affect the stability of line infrastructure in horizontal direction [19]. The main goal for this study is therefore to develop methods to estimate the stability of line infrastructure in the vertical and horizontal directions, and offer some new standard InSAR products accordingly, and describe the performance assessment metrics for line infrastructure monitoring.

2. METHODS

A SAR satellite delivers line-of-sight (LOS) measurements over line infrastructure. Here we first introduce the concept of the LOS-vector decomposition to a local, asset-fixed coordinate system when two or more SAR satellite observations are available. To connect all SAR measurements, we address a method to align all the LOS-vector measurements over line infrastructure to a unique coordinate, and then we discuss the quality of the LOS-vector decomposition via 3D (co)variance matrix and the Dilution of Precision (DoP). The performance assessment metrics, i.e. sensitivity circle, are also presented.

2.1. LOS-vector decomposition

The mathematic model for LOS-vector decomposition is defined as [19],

$$E\{\underbrace{\begin{bmatrix}\underline{d}^{(1)}_{\text{LOS}}\\ \underline{d}^{(2)}_{\text{LOS}}\\ \underline{d}_L\end{bmatrix}}_{\underline{d}'}\} = \underbrace{\begin{bmatrix}p_{11} & p_{12} & p_{13}\\ p_{21} & p_{22} & p_{23}\\ 0 & 1 & 0\end{bmatrix}}_{A}\underbrace{\begin{bmatrix}d_T\\ d_L\\ d_N\end{bmatrix}}_{d_{\text{asset}}};$$

$$D\{\underbrace{\begin{bmatrix}\underline{d}^{(1)}_{\text{LOS}}\\ \underline{d}^{(2)}_{\text{LOS}}\\ \underline{d}_L\end{bmatrix}}_{\underline{d}'}\} = \underbrace{\begin{bmatrix}\sigma^2_{d,\text{LOS},1} & 0 & 0\\ 0 & \sigma^2_{d,\text{LOS},2} & 0\\ 0 & 0 & \sigma^2_{d,L}\end{bmatrix}}_{Q_{d'}}, \quad (1)$$

where $E\{.\}$ and $D\{.\}$ express the expectation and dispersion operator, respectively. Two LOS-vector measurements with different viewing geometries are denoted by $\underline{d}^{(1)}_{\text{LOS}}$ and $\underline{d}^{(2)}_{\text{LOS}}$, and the underline indicates the stochastic nature of the observations. The observation-vector, $\underline{d}'$, also contains the pseudo-observation $\underline{d}_L$, which is set to zero if no other information is available. d_{asset} represents the estimated vector in the local, asset-fixed coordinates, including the components d_T, d_L, d_N in transversal, longitudinal, and the complementing normal direction, respectively. $p_{i,j},\ i,j \in [1,2,3]$ are the elements of the projection vector. Notes that the projection vector is a function of satellite heading, satellite incidence angle, line-infrastructure heading direction β_a, longitudinal and transversal slope of line-infrastructure, more detail in [1].

2.2. 3D (co)variance matrix

According to error propagation law, the precision of LOS-vector decomposition (see Eq. (1)) can be described via the covariance matrix of $\underline{\hat{d}}_{\text{asset}}$,

$$Q_{\hat{d}_{\text{asset}}} = (A^T Q^{-1}_{d'} A)^{-1} = \begin{bmatrix}\sigma^2_T & \sigma_{TL} & \sigma_{TN}\\ \sigma_{LT} & \sigma^2_L & \sigma_{LN}\\ \sigma_{NT} & \sigma_{NL} & \sigma^2_N\end{bmatrix}, \quad (2)$$

where the subscripts T, L, and N are shorthand notation for the deformations in the asset-fixed coordinate system.

2.3. Dilution of Precision

An alternative quality metric is the Dilution of Precision (DoP). It can be defined as [20]

$$\text{DoP} = (\det(Q_{\hat{d}_{\text{asset}}}))^{\frac{1}{2n}}, \quad (3)$$

where det(.) is the determinant operator. Having more SAR satellites, the result quality is improved if the DoP value reduces.

2.4. Performance assessment metrics: sensitivity circle

The scalar sensitivity metric $s \in [0,1]$ is associated to one specific deformation direction, indicated in a 3D Euclidian space by unit vector $\vec{d}_{\text{asset}}$, given the line-of-sight unit vector $\vec{l}$ from the target to the sensor. It is defined as the inner product of both,

$$s = \left|\vec{d}_{\text{asset}} \cdot \vec{l}\right|, \quad (4)$$

which is the orthogonal projection of $\vec{d}_{\text{asset}}$ on $\vec{l}$. The metric is useful to assess whether asset deformation in a specific (expected) direction is observable with a specific satellite. For line-infrastructure, assuming orthogonal and normal (vertical) deformations only, we introduce *sensitivity circles*, see Fig 1.

We project the unit deformation vector onto the LOS directions of a number of satellites, with different satellite headings and satellite incidence angles, using Eq. (1). Considering the possible local heading directions of the asset, the *orthogonal elevation angle*, ζ, of the unit deformation vector can vary in the range $(-180°, 180°]$ in a plane orthogonal to the local line-infrastructure heading direction, e.g. the rail track direction, see the sketch in the middle of Fig. 1. The angle $\zeta = 0°$ corresponds with a horizontal deformation looking right when facing the asset azimuth (heading) direction of the line-infrastructure, while $\zeta = \pm 180°$ means leftward-looking horizontal deformation. If $\zeta = +90°$, it implies upward vertical deformation. Since the LOS-vector sensitivity values are line-symmetric for a full cycle when $\zeta \in (-180°, 180°]$, we plot the LOS-vector sensitivity circle only in the range $\zeta \in [0°, 180°]$.

Fig. 1 demonstrates the sensitivity circles for one particular location along a line-infrastructure segment, in this case a location along a railway. For example, in Fig. 1a), the railway track is heading northbound, while in Fig.1b), the heading is eastbound. The two colored semi-circles show the sensitivity values, s, for each of the satellites available for this particular asset. A sensitivity of $s = 1$ implies that the geometric quality for that particular deformation vector direction is optimal, while zero sensitivity relates to a deformation vector which is in the null-space of that particular satellite. Thus, a deformation in that particular direction will be not detectable. The sensitivity circle for, e.g., Radarsat-2 ascending (the outermost semi-circle in the plots) indicates a sensitivity value of 0.83 for vertical upward (or downward) deformation. Quantitatively this implies that the standard deviation of the LOS deformation estimates, given the asset azimuth β_a, needs to be divided by this sensitivity value, $\sigma_\zeta(\zeta|\beta_a) = \sigma_{d,\text{LOS}}/s(\zeta)$.

The combination of all available satellite data sets (in this case four) allows us to assess whether a particular deformation can be observed and to which precision. Comparing Figs. 1a) and b), it can be observed that for an eastbound infrastructure heading, cf. Fig. 1b), the alignment of the blue areas indicates that a left- or right-lateral deformation will be

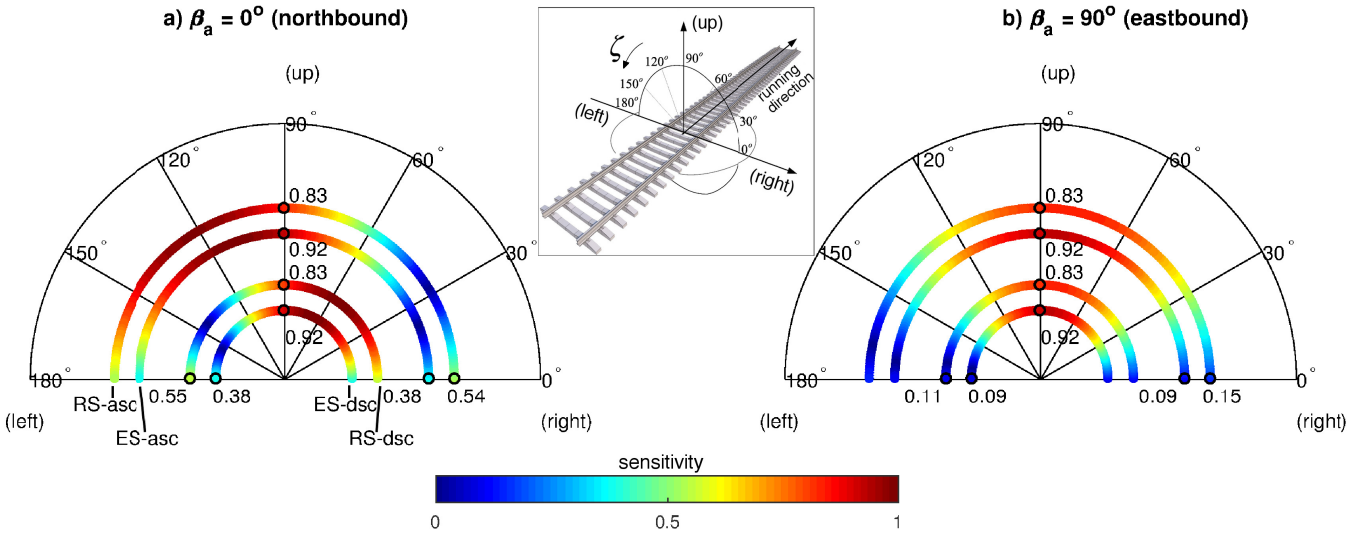

Fig. 1. LOS-vector sensitivity circles for given asset azimuth angle values of line-infrastructure a) $\beta_a = 0°$, b) $\beta_a = 90°$. Four rings from outer to inner represent the LOS-vector sensitivity for Radarsat-2 in ascending orbit (RS-asc), Envisat in ascending orbit (ES-asc), Radarsat-2 in descending orbit (RS-dsc), and Envisat in descending orbit (ES-dsc), respectively. The orthogonal elevation angle ζ of the unit deformation vector direction is confined in $[0° \ 180°]$. The color represents the scaled sensitivity between $[0 \ 1]$. The sketch in the middle describes the viewing of the orthogonal elevation angle of the unit deformation vector.

nearly impossible to detect, as the LOS-sensitivities are all minimal in that direction.

3. CASE STUDY: PRODUCTS AND PERFORMANCE ASSESSMENT METRICS FOR LINE INFRASTRUCTURE MONITORING

In this work, we develop some new products for line infrastructure monitoring: i) significant deformation maps, ii) longitudinal anomaly profiles, iii) transversal-normal decomposition. We also present the particular performance assessment metrics: the DoP and LOS-vector sensitivity maps along line infrastructure. Relevant results and discussion for a Dutch railway line infrastructure asset will be shown in our full paper. More details refer to [1].

4. CONCLUSIONS

Operational monitoring of the stability of line infrastructure benefits from the synergistic application of InSAR using multiple satellite missions. Differences in the orbital and instrumental viewing geometry, as well as spatial and temporal coverage and resolution, optimize the amount of information that can be extracted from the data. A generic mathematical framework was introduced to enable a decomposition of radar measurements in the normal (vertical) and transversal direction of the railway. This includes a sensitivity, precision analysis, and performance assessment. New products and performance assessment metrics for line infrastructure monitoring are presented and demonstrated on the Dutch railway line infrastructure asset.

5. REFERENCES

[1] Ling Chang, Rolf P.B.J. Dollevoet, and Ramon F. Hanssen, "Monitoring line-infrastructure with multisensor SAR interferometry: products and performance assessment metrics," *IEEE journal of selected topics in applied earth observations and remote sensing*, vol. 11, pp. 1593–1605, 2018.

[2] U Soergel, E Cadario, A Thiele, and U Thoennessen, "Feature extraction and visualization of bridges over water from high-resolution InSAR data and one orthophoto," *IEEE Journal of Selected Topics in Applied Earth Observations and Remote Sensing*, vol. 1, no. 2, pp. 147–153, 2008.

[3] L Chang and RF Hanssen, "Detection of permafrost sensitivity of the Qinghai–Tibet Railway using satellite radar interferometry," *International Journal of Remote Sensing*, vol. 36, no. 3, pp. 691–700, 2015.

[4] L. Chang, R. Dollevoet, and R. F. Hanssen, "Nationwide railway monitoring using satellite SAR interferometry," *IEEE Journal of Selected Topics in Applied Earth Observations and Remote Sensing*, vol. PP, pp. 1–9, 2016.

[5] Richard Bamler and Philipp Hartl, "Synthetic aperture

radar interferometry," *Inverse problems*, vol. 14, no. 4, pp. R1–54, 1998.

[6] Ramon F Hanssen, *Radar Interferometry: Data Interpretation and Error Analysis*, Kluwer Academic Publishers, Dordrecht, 2001.

[7] Alessandro Ferretti, Claudio Prati, and Fabio Rocca, "Nonlinear subsidence rate estimation using permanent scatterers in differential SAR interferometry," *IEEE Transactions on Geoscience and Remote Sensing*, vol. 38, no. 5, pp. 2202–2212, Sept. 2000.

[8] Andrew Hooper, "A multi-temporal InSAR method incorporating both persistent scatterer and small baseline approaches," *Geophysical Research Letters*, vol. 35, no. 16, 2008.

[9] Yuri Fialko, Mark Simons, and Duncan Agnew, "The complete 3-D surface displacement field in the epicentral area of the 1999 mw7. 1 hector mine earthquake, california, from space geodetic observations," *Geophysical Research Letters*, vol. 28, no. 16, pp. 3063–3066, 2001.

[10] Tim J Wright, Barry E Parsons, and Zhong Lu, "Towards mapping surface deformation in three dimensions using InSAR," *Geophysical Research Letters*, vol. 31, 2004.

[11] D L Galloway, K W Hudnut, S E Ingebritsen, S P Phillips, G Peltzer, F Rogez, and P A Rosen, "Detection of acquifer system compaction and land subsidence using interferometric synthetic aperture radar, Antelope Valley, Mojave Desert, California," *Water Resources Research*, vol. 34, no. 10, pp. 2573–2585, 1998.

[12] Falk Amelung, Devin L Galloway, John W Bell, Howard A Zebker, and Randell J Laczniak, "Sensing the ups and downs of Las Vegas: InSAR reveals structural control of land subsidence and aquifer-system deformation," *Geology*, vol. 27, no. 6, pp. 483–486, June 1999.

[13] Ling Chang and Ramon F Hanssen, "Detection of cavity migration and sinkhole risk using radar interferometric time series," *Remote Sensing of Environment*, vol. 147, pp. 56–64, 2014.

[14] Estelle Chaussard, Shimon Wdowinski, Enrique Cabral-Cano, and Falk Amelung, "Land subsidence in central Mexico detected by ALOS InSAR time-series," *Remote sensing of environment*, vol. 140, pp. 94–106, 2014.

[15] Yuri Fialko, "Interseismic strain accumulation and the earthquake potential on the southern San Andreas fault system," *Nature*, vol. 441, no. 7096, pp. 968–971, 2006.

[16] Noel Gourmelen, Falk Amelung, Francesco Casu, Mariarosaria Manzo, and Riccardo Lanari, "Mining-related ground deformation in crescent valley, nevada: Implications for sparse gps networks," *Geophysical Research Letters*, vol. 34, no. 9, 2007.

[17] Wei-Chia Hung, Cheinway Hwang, Yi-An Chen, Chung-Pai Chang, Jiun-Yee Yen, Andrew Hooper, and Chin-Yi Yang, "Surface deformation from persistent scatterers SAR interferometry and fusion with leveling data: A case study over the Choushui River Alluvial Fan, Taiwan," *Remote Sensing of Environment*, vol. 115, no. 4, pp. 957–967, 2011.

[18] Tore Dahlberg, "Some railroad settlement models—a critical review," *Proceedings of the Institution of Mechanical Engineers, Part F: Journal of Rail and Rapid Transit*, vol. 215, no. 4, pp. 289–300, 2001.

[19] L. Chang, R.P.B.J Dollevoet, and R.H Hanssen, "Railway infrastructure monitoring using satellite radar data," *The International Journal of Railway Technology*, vol. volume 3, pp. 79–91, 2014.

[20] P J G Teunissen and D Odijk, "Ambiguity dilution of precision: concept and application," in *In: proc. ION-97, 16-19 September, Kansas City, USA, pp. 891-899*, 1997.